Fullerene-Based Organic−Inorganic Nanocomposites and Their Applications

Plinio Innocenzi* and Giovanna Brusatin

Dipartimento di Ingegneria Meccanica, Settore Materiali, Università di Padova, Via Marzolo 9, 35131 Padova, Italy

Received February 1, 2001

The development of new materials based on the novel and unique properties exhibited by the family of fullerenes is attracting growing interest from materials scientists. As the progress of the studies discloses new properties and basic knowledge is better established, three main fields are emerging in the preparation of materials from fullerenes: fullerene thin films, organic polymeric materials that contain fullerene molecules, and the incorporation of fullerenes and their derivatives in inorganic host matrixes to fabricate organic−inorganic nanocomposites. This last family of materials, in particular, opens several interesting perspectives for different applications, especially in nonlinear optics and photoelectrochemistry. Fullerene organic−inorganic nanocomposites have been prepared using porous media as a host matrix and different groups of materials synthesized via sol−gel, such as aerogels, porous inorganic oxides, and hybrid and mesoporous materials. Nanocomposite materials developed from fullerenes in inorganic host media are the objects of the present review.

1. Introduction

Immediately after the discovery[1] of C_{60} and the development of a large-scale production method,[2] the attention of materials scientists has been attracted by the synthesis of new materials based on the family of fullerene molecules. Many properties of fullerenes are, in fact, new or unusual,[3−5] and with a better understanding of their chemical and physical properties[6] the fabrication of new materials for advanced applications has emerged as a challenging possibility.

The family of fullerene materials can be divided in three main groups, materials such as Langmuir−Blodgett films, self-assembled monolayers and thermally evaporated or solution cast films, which are directly obtained by fullerene molecules and their derivatives in the form of thin films.[7] All-organic materials, where fullerenes are embedded or linked to a polymeric organic matrix, compose another group.[8] The third group of fullerene-based materials is represented by organic−inorganic nanocomposites obtained by incorporating fullerene molecules and their derivatives in an inorganic matrix. Fullerenes are introduced without any direct bond with the matrix network or grafted to the backbone using properly functionalized fullerenes. Several difficulties have, however, challenged the materials scientists to develop this type of nanocomposite materials, such as the low solubility of fullerene in organic solvents and the difficult control of the aggregation state of fullerenes. The final properties of the material have appeared to be strictly linked to the state of the fullerenes, in fact, totally different properties have emerged if fullerenes are incorporated as isolated molecules, clusters or larger aggregates. Another important feature to be considered is the close relationship of several fullerene properties with the environment. Not only the aggregation state but also the nature of the surrounding media heavily affects the physical−chemical properties of fullerenes. Many efforts have been, therefore, addressed to reach a full control of the state of the doping molecule inside the host matrix and to develop new strategies to entrap fullerenes.

A first solution is offered by porous inorganic materials that can be easily impregnated by C_{60} in suitable solvents. Porous materials, however, have limited applications and cannot be processed as coating layers. Other attracting host media are sol−gel materials because of their low processing temperature and the very flexible soft chemistry that allows a very fine-tuning of the matrix properties. Several groups of sol−gel materials have appealing properties to buildup fullerene nanocomposites, among them, aerogels, organic−inorganic hybrids, inorganic porous oxides, and self-assembled mesoporous materials. In this paper the current literature on fullerene organic−inorganic nanocomposites is rewieved; all the materials formed by an inorganic or organic−inorganic host matrix with embedded or grafted fullerenes and their derivatives have been here discussed.

2. Porous Inorganic Host Materials

The introduction of organic molecules in inorganic porous materials represents a relatively simple and widely applied process to obtain organic−inorganic nanocomposites. Combining one of the several available porous host media with a suitable doping method gives enough flexibility to adjust, within a certain extent, the properties of the final material. Some attention has, therefore, been devoted to fullerene nanocomposites based on porous inorganic materials as host matrix. Even if the low solubility of fullerenes in polar solvents represents a limit, especially impregnation, and the control of the aggregation states within the matrix is

* To whom correspondence should be addressed.

10.1021/cm0110223 CCC: $20.00
Published on Web 10/15/2001

difficult to achieve, several examples have been reported. Much of the research has been addressed to study the interaction of fullerenes with the host matrix or to obtain materials with new or improved photoluminescence properties.

In this section the current literature on fullerene organic−inorganic nanocomposites fabricated from porous material is rewieved. The attention has been focused on the host materials more than the different doping methods; in fact, the differences in some peculiar properties of the matrix, such as pore dimension, surface area, chemical nature of the pore walls, etc., are by far the most important parameter to affect the nanocomposite material.

2.1. C_{60} in Zeolites. The family of zeolites is composed of nanoporous materials with pores generally in the range 0.3−1.3 nm. The intriguing feature of using zeolites as host matrix of fullerenes is their pore dimensions that are very close to the 0.88 nm diameter of C_{60}. Zeolites with pores larger than 1 nm allow fullerene diffusion into the pores and have enough space to accommodate it. C_{60} molecules will be confined in a monodimensional array within a nanoporous inorganic host material.

The first incorporation of C_{60} in a molecular sieve was reported by Keizer[9] et al., who inserted, by a vacuum evaporation method, a very small amount of C_{60}^- into 13X. Interesting results were obtained upon incorporation of C_{60} in VPI-5 zeolites, which are nanoporous aluminophosphate crystalline materials with a hexagonal arrangement of monodimensional pores of 1.25 nm diameter. The microstructure is formed of alternating corner-sharing AlO_4 and PO_4 tetrahedra linked together to give a monodimensional 18-atom ring channel, and fullerenes incorporated within this structure should form a monodimensional array. C_{60} was introduced into VPI-5 via impregnation of solutions of benzene,[10−13] or from the gas phase. Gügel[14] et al. reported the successful incorporation of C_{60} in $AlPO_4$-8 from gas phase but failed with $AlPO_4$-5, apparently because the pore opening is too small to allow absorption of fullerenes. C_{60} is introduced after the preparation of the host material, by impregnating the zeolites with C_{60} in benzene. Several experiments confirmed that C_{60} molecules are truly incorporated within the pore structure of the zeolites. In particular, the presence of C_{60} within the pores is confirmed by suppression of the phase transition of VPI-5 to $AlPO_4$-8 observed upon heating.[15] This phase change is due to constriction of the pore structure into the 14-ring of aluminophosphate $AlPO_4$-8 and is inhibited by the incorporation of C_{60} that stabilizes the pore structure. A comparative study[12] of differential thermal analysis−thermogravimatric analysis (DTA−TGA) data from undoped and fullerene-doped VPI-5, prepared by the Anderson method,[10] gives an approximate stoichiometry of 1 C_{60} for 35 $AlPO_4$ units, which corresponds in average to 1 C_{60} molecule in the matrix every 1.5 nm or a two-thirds filling level of the pores.

The incorporation into the zeolites of isolated C_{60} results in a clear modification of the fullerene electronic structure. The C_{60}-matrix interaction gives novel characteristics, in particular photoluminescence emission of white light at room temperature and shifts in the optical absorption peaks.[11]

Optical absorption measurements on C_{60}−VPI-5 nanocomposite materials show a red shift of the absorption maxima in comparison to C_{60} in *n*-hexane solutions. Absorption red shift is also observed after incorporation of C_{60} in sol−gel materials,[16−18] or polymers[19] and there is a general agreement to attribute this effect to the interaction of C_{60} with a more polar interface. Comparing the red shift of C_{60} in VPI-5 with those in other media, the cage of the zeolites can be considered as a high-polarity environment. The interaction of fullerene molecule with oxygen atoms in the zeolites pore walls produces a partial mixing of electrons density. The VPI-5 cage is supposed to induce a symmetry breaking in C_{60} that produces electronic transitions otherwise forbidden in isolated fullerenes.

In general the UV−visible absorption spectra exhibited by C_{60}[20] and its derivatives are quite sensitive to the environment, and a dependence on solvent[21] and solute aggregation states was observed.[22] C_{60} in *n*-hexane has characteristic absorption bands peaking around 210, 260, and 330 nm[22] corresponding to 8^1T_{1u}, 6^1T_{1u}, and 3^1T_{1u} transitions to the excited state, respectively. These bands, together with the vibronic absorptions in the 400−410 nm region, are indicative of the C_{60} interaction with the environment, while the band at 450 nm is attributed to the formation of aggregates. In fullerene derivatives the same bands are slightly shifted[17,23] but a similar dependence on the environment is reported.[17] After incorporation in a host, matrix shifts of the absorption maxima in the 200−400 nm region are attributed to changes in the polarity environment, while the intensity of the 450 nm peak gives a direct indication on the presence of fullerenic aggregates within the matrix. When C_{60} is located near a polar interface, the absorption maxima is red shifted with respect to C_{60} in *n*-hexane or toluene, while a less polar environment produces a blue shift.

Photoluminescence (PL) is another photophysical property of fullerenes that revealed a strong dependence on environment and aggregation state, upon incorporation in a solid matrix. In crystalline C_{60} the transition in the 1.9 eV energy gap between the highest occupied molecular orbital (HOMO) and the lowest unoccupied molecular orbital (LUMO) is forbidden and C_{60} is very weakly photoluminescent at room temperature;[24,25] only at very low temperature, as for instance the liquid helium temperature, can photoluminescence be clearly detected.

After incorporation in VPI-5 zeolites, remarkable changes in the fluorescence spectrum are observed.[10−13] The main peak in the 1.7 eV region, due to emission in crystalline powders, broadened, increased in intensity, and extended to the visible region, peaking around 2 eV. The material becomes a white-light emitter with fluorescence detectable even at room temperature by naked eye.[11] The PL spectra of C_{60} doped and undoped VPI-5 are shown in Figure 1, reprinted from ref 12.

In the 830−540 nm interval a set of five lifetimes,[12,13] with 10−80 ps, 180 ps, 450 ps, 1.2 ns, and 4.6 ns, in VPI-5 doped with C_{60}, is observed. After comparison with fluorescence from the zeolite matrix and solid C_{60}, only the 1.2 ns lifetime was unambiguously attributed to emission from confined C_{60} molecules in the pores. This supports the indication that C_{60} is incorporated

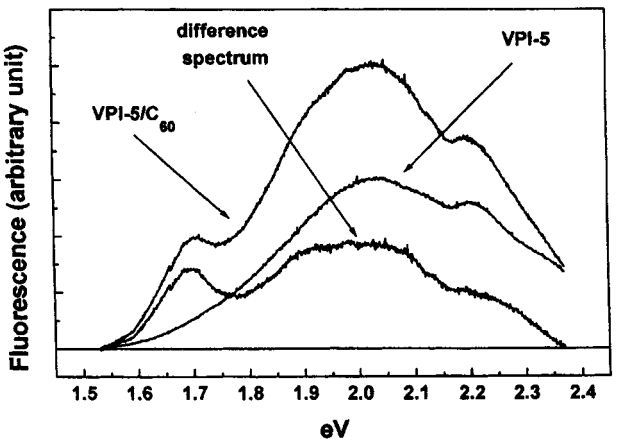

Figure 1. Photoluminescence spectra of VPI-5 doped with C_{60} molecules, VPI-5, and the difference spectrum ($\lambda_{ex} = 532$ nm). Reprinted with permission from ref 12. Copyright 1998 Elsevier.

within the zeolites mainly as a single molecule. A lifetime of 1.2 ns is close to the value measured for C_{60} in toluene,[26] and the broadening of the spectrum, with respect to solid C_{60}, after incorporation in VPI-5 is also similarly observed in solution, when C_{60} molecules do not interact with each other.

Following the experiment of Keizer,[9] the PL of C_{60} in 13X zeolites was investigated by Gu[27] et al. A regular framework of corner sharing SiO_4 and AlO_4 tetrahedra that form a three-dimensional network of pores and cages composes 13X zeolites. The pores are linked to spherical cages called supercages. The average pore size is about 0.75 nm, while the supercage has larger dimensions, around 2.4 nm in length and 1.3 nm in diameter. Fullerenes are introduced by evaporation in nitrogen gas and occupied preferentially the positions in the supercages due to their larger dimensions. The interesting feature of using zeolites of the type of 13X as host matrix for C_{60} is represented by their charged nature. While VPI-5 zeolites are not electrically charged, and so do not require any compensating charge, each aluminum ion in 13X needs a compensating Na^+ cationic charge. The charged surface of 13X induces a strong interaction with the guest fullerenes. The presence of C_{60}^- species in 13X molecular sieves is confirmed by electronic paramagnetic resonance (EPR) signals. Fullerenes within the 13X supercages are strongly polarized because the delocalized π electrons interact with the electric charges on the pore walls and charge transfer processes can easily occur, generating a C_{60} anion.

The PL spectrum of C_{60} confined in NiY zeolites[28] shows a strong PL response at 544 nm, attributed to fullerenes, and a weaker emission at 516 nm, resulting from Ni ions of the NiY zeolites. The PL emission is sensitively shifted to larger energies with respect to C_{60} in 13X,[27] because of the presence of coordinating Ni ions on C_{60}. The fullerenes are mainly entrapped within the supercages, as in the case of 13X zeolites, and anchored to the pore walls via the Ni ions that covalently interact with C_{60} molecules. This interaction is responsible of the carrier transfer effect that induces a structural modification in C_{60} and causes the strong PL response of confined fullerenes within NiY zeolites.

An interesting application of zeolites as reactors for selective functionalization of fullerenes was patented by Zhenyu[29] et al. L, ETS-10, and NaY zeolites were impregnated with a solution of C_{60} in benzene, and the fullerene-loaded zeolites were placed in a reaction room where chlorine gas was introduced to carry out a photochlorination by UV irradiation or thermal chlorination by thermal treatment. The fullerenes that were chlorinated while on the molecular sieve show over 50% disubstituted and 70% tetrasubstituted of the reaction products. This is a much larger amount of selective fullerene derivatives with respect to a process of thermal chlorination performed outside the molecular sieve.

It is noteworthy to observe, concluding the description of fullerenes in zeolites, and even if fullerene nanotubes[30] are not the object of the present review, that zeolites because of their monodimensional channels are also an ideal host matrix and template for carbon nanotubes. The synthesis of single-wall carbon nanotubes (SWCNT), which are formed by a layer of graphite rolled-up into a cylindrical shape, in the one-dimensional channels of zeolites represents an interesting strategy to obtain aligned SWCNT.[31]

2.2. Fullerenes in Self-Assembled Mesoporous Materials. Mesoporous materials are a class of materials with pores in the range 2−50 nm, generally synthesized using a self-assembling process in the presence of surfactants.[32] Materials with different oxide compositions such as powders, self-standing films, and, more recently, supported thin films can be produced.[33] The mesoporous materials are usually indicated by an acronym, such as MCM (mobile catalytic materials) followed by a letter to specify the class of symmetry, i.e., hexagonal (MCM-41), cubic (MCM-48), and lamellar (MCM-50). Another group of mesoporous materials is formed by folded mesoporous materials[34] (FSM)-16 that have a honeycomb mesophase with ordered cylindrical channels of 2−10 nm in diameter. The dimensions of the pores are larger than those in zeolites, and these materials are, therefore, an interesting host matrix for fullerene molecules. Furthermore, mesoporous materials possess very large and easily accessible surface areas, with uniform pore sizes and topologies. MCM-41,[35−39] MCM-48,[40] and FSM-16,[41−43] fullerene nanocomposites were prepared by different research groups. Different methods were employed to introduce fullerenes in the mesoporous matrix, adsorption from a toluene solution of C_{60},[38−40,44] sublimation,[35,43] vapor transport,[36] and grinding together a mixture of C_{60} and calcined MCM-41.[37] Fullerenes were always introduced in a material in a postpreparation approach, no attempts to use any specific fullerene derivatives to be grafted to the pore walls have been yet reported.

An interesting experiment, where mesoporous materials are used to test supramolecular complexation of C_{60}, was reported by Drljaca[44] et al. In general, the formation of C_{60} complexes in solution, for instance by cyclotriveratrylenes or hydrophobic calixarenes, is difficult to identify, because of the very weak intermolecular interactions involved. Entrapping C_{60} together with complexing agents within a mesoporous matrix can stimulate the host−guest interactions in the complex allowing an easier identification of the supramolecular complexes. The pore size, 5.4 nm in radius, of the silica host material used in the experiment, allows the mobilization of C_{60} and is large enough to accommodate

fullerene aggregates together with the associated host molecules. The reflectance UV−vis absorption spectra of the mesoporous silica impregnated with toluene solutions of C_{60} show the typical pattern of C_{60} solvated by toluene.[22] After removal of the residual toluene within the pores, fullerene aggregates are formed. The formation of aggregates is, however, a reversible process as shown by the disappearing of the 450 nm band after new impregnation in toluene. When the material is, however, impregnated with calixarene or cyclotriveratrylene in toluene, the absorption band at 450 nm is clearly detected indicating the presence of fullerene aggregates. These clusters are attributed to micelle-like structures with a fullerene core surrounded by host molecules in the pores.

The adsorption of C_{60} on MCM-41, from toluene solutions at room temperature under dynamic conditions, was studied by flow microcalorimetry.[38] The fullerene adsorption was completely reversible, and the adsorbed amount is very small even at equilibrium concentrations close to the solubility limit. The adsorbed C_{60} molecules occupy only a very small fraction of the total MCM-41 surface area, at least in the reported experimental conditions.

The optical properties of C_{60} confined into 3 nm hexagonal channels of MCM-41 were studied by Gu[36] et al. C_{60} was introduced in the mesopores, similar to introduction in zeolites,[27] by a vapor transport method using nitrogen as transport gas. The PL spectrum shows two intense photoluminescence peaks around 484 and 642 nm, while undoped MCM-41 does not show PL emission. The PL response at 642 nm is attributed to fullerenes entrapped in MCM-41. The origin of the 484 nm PL, instead, is explained by passivation of MCM-41 pores induced by C_{60} during the doping process. The pore walls in MCM materials, even after calcination, are rich in hydroxyl groups that can be used to graft functional molecules[33] and that are polar reactive sites. Strong interaction of C_{60} with the pore walls after entrapping must be therefore expected, as confirmed by Govindaraj[40] et al. who observed C_{60}-doped MCM-48 passivation of the pores, attributed to C_{60}−Si, C_{60}−OSi, C_{60}−OH, and C_{60}−H bonding. The PL spectra of C_{60}−MCM-48 show two emission bands, a weak band at 1.8 eV due to C_{60} and a broader band around 2.2 eV due to the matrix. An increased concentration of fullerenes in MCM-48 produces a sensitive change in the PL spectra, with an increase in intensity in the band at 1.8 eV and a little blue shift in the 1.8−1.9 eV region. At the same time the band at 2.2 eV decreases in intensity and becomes broader. A similar quenching effect of the matrix fluorescence produced by fullerenes has been also observed in C_{60}-doped aerogels. The interaction of C_{60} with the MCM pore walls is, therefore, an important feature in the synthesis of MCM-C_{60} nanocomposites. Infrared studies on the dehydroxylation of C_{60}-loaded MCM-41[37] show a different behavior. It was postulated that C_{60} during the calcination process to remove the template is able to capture the hydroxyls from silanols, Si−OH, in MCM-41 pore walls to form C−H and C−OH species that actually condense.

Upon incorporation of C_{60} in MCM-41, quantum size effects due to the formation of C_{60} clusters confined within the mesopores must be expected. The pore size

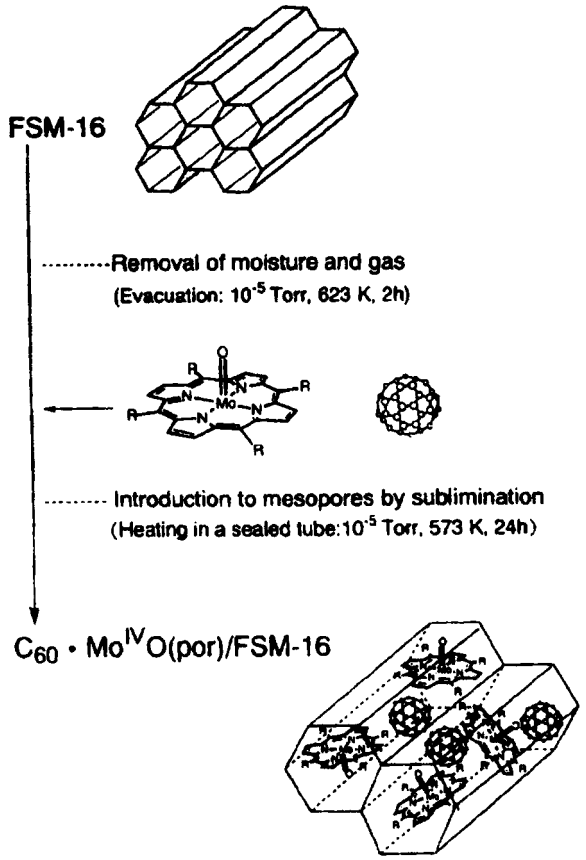

Figure 2. Procedure of preparation of C_{60}.$Mo^{IV}O$(tpp)/FSM-16 nanocomposites. Reprinted with permission from ref 43. Copyright 1998 Elsevier.

in mesoporous materials is in fact much larger than that in zeolites, where the pore dimensions hardly exceed the diameter of fullerenes, and clusters composed of few fullerene molecules are likely to be formed. Electronic spin resonance (ESR) experiments[35] gave a clear evidence of the discrete character of the electronic band structure of quantum-confined C_{60} in the channels of MCM-41 materials.

Another different group of supramolecular hybrid nanocomposites can be prepared introducing by sublimation metalloporphyrins (oxomolybdenum(IV) tetraphenylporphyrins ($Mo^{IV}O$(tpp)) or ferro(II) tetraphenylporphyrins (Fe^{II}(tpp)) or C_{60}[43] into the ordered nanochannels of FSM-16. The dopants are highly dispersed and homogeneously entrapped in the mesoporous channels to form supramolecular hybrids C_{60}•$Mo^{IV}O$-(tpp)−FSM-16 and C_{60}•Fe^{II}(tpp)−FSM-16 (Figure 2).

The interesting property of these nanocomposites is their ability to uptake O_2 and the catalytic oxygen transfer function between MO or Fe porphyrins and fullerenes in FSM-16. The additional inclusion of fullerenes in $Mo^{IV}O$(tpp)−FSM-16 substantially increases the oxygen uptake, with respect to $Mo^{IV}O$(tpp)−FSM-16 itself. The action of C_{60} as oxygen carrier to promote the isolation of $Mo^{IV}O$(tpp) inside the mesopores and the formation of O_2 adduct complexes, is suggested to explain the result. The nanocomposites show also interesting photocatalysis properties for selective propene oxidation toward acetone.

2.3. C_{60} in Porous Silicon. Porous silicon, because of its open pore structure and very large specific surface

area, represents an interesting medium to be used as host matrix of C_{60}.[45,46] While several papers investigated the adsorption of fullerenes on silicon surfaces (see for instance Yamaguchi[47] et al. and references therein), only a few were dedicated to study the adsorption on the pores in porous silicon.

Yan[45] et al. introduced C_{60} into a 20 mm thick layer of microporous silicon obtained by electrochemical etching on the surface of a silicon layer. Two different methods were employed to embed the guest molecules, impregnation by a C_{60}−toluene solution and covalently tethering of fullerenes to the silicon pore wall by CH_3-$(C_2H_3O)_2Si(CH_2NHCH_2CH_2NH_2)$ as silane coupling agent. C_{60} survives in the porous silicon, after washing, in different states, adsorbed to the pore walls or as polycrystalline aggregates. The room-temperature PL of C_{60} in porous silicon is clearly enhanced; the PL spectra reveal three distinct peaks, at 730 nm associated to polycrystalline C_{60}, at 620 nm due to adsorbed fullerene on the silicon wall, and at 630 related to C_{60} tethered molecules. The observed enhancement of PL is attributed to a carrier transfer effect from porous silicon crystallites, which play the role of a carrier generator, to C_{60} molecules that behave as radiative recombination centers.[45] Raman scattering experiments[46] showed that charge transfer of at least two electrons per C_{60} molecule occurs. Different shifts in the Raman spectra also revealed that there is stronger bonding, and therefore a greater electron transfer to C_{60}, when fullerenes are electrochemically bonded to the silicon wall by the coupling agent.

2.4. Fullerene−Aerogel Nanocomposites. Aerogels are a class of porous materials with novel and unique properties.[48] They are characterized by ultralow density, open pore structures, and surface areas usually in the range 150−900 $m^2 \cdot g^{-1}$. Monolithic materials with porosities of the order of 90−95% are easily obtained. Aerogels are also used as a host matrix for functional organic molecules and nanoparticles to prepare a large variety of nanophasic materials. A common procedure to fabricate aerogels combines sol−gel processing with supercritical extraction of the solvent. A dry, low-density material is produced with the composition of different oxides with silica being the most common. A guest molecule can be introduced in the aerogel during the synthesis of the gel, before the supercritical solvent extraction.

The first fullerene−aerogel nanocomposite was prepared by Bell et al.[49] A water-soluble fullerene−ethylenediamine and a fullerene−silane derivative soluble in organic solvents have been introduced in silica aerogels. The advantage in using soluble derivatives, with respect to pristine C_{60}, is given by the larger amount of fullerenes that are introduced in the final material and the better control of aggregation states within the matrix. The aerogels can be loaded up to 9% of fullerenes in weight.

A simpler approach was followed by Shen et al.,[50−53] to introduce C_{60} and a C_{60}/C_{70} mixture in silica aerogels. C_{60} is dissolved in toluene and added to an acid catalyzed sol of TEOS. The concentration of C_{60} in the silica gel is limited by the low solubility in toluene and remains in the range 0.001−0.5 mol %. After several days of aging, the gels are dried in supercritical conditions. The C_{60}/C_{70} mixture is, instead, introduced directly in the sol that is sonicated to reach a homogeneous fullerene distribution. The introduction in silica aerogels of C_{60} or C_{60}/C_{70} mixtures, following these procedures mainly produces fullerenes clusters that give rise to quantum confinement effects (QCE) and the emission of intense visible light. As previously observed, in normal conditions fullerene powders exhibit only a very weak photoluminescence[25] peaking around 1.7 eV. In aerogels, intense visible light emissions around 2.1 and 2.3 eV are observed. The luminescence results also increased in intensity and shifted toward blue. These effects are attributed to HOMO−LUMO transitions in C_{60}, which are usually forbidden by the selection rules, and therefore, the PL in fullerene powders is very low. The excited electrons and holes immediately relax to the bottom of the conduction band and to the top of the valence band, respectively. The little fullerene clusters formed with the incorporation in aerogels give rise to a quantum dot effect that produces a blue shift and a larger quantum yield of photoluminesce. This effect is confirmed by the observed reduction in the quantum yield at larger doping concentrations of fullerenes, which should give larger clusters, because[52] (Figure 3) of the QCE weakening that is inversely proportional to the size of a quantum dot.

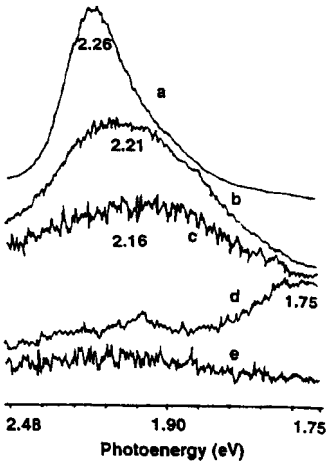

Figure 3. Photoluminescence spectra of silica aerogels doped with C_{60}/C_{70} mixtures as a function of concentration: (a) 0.05 mol %; (b) 1.25 mol %; (c) 2.5 mol %; (d) pristine C_{60}/C_{70}. Argon laser excitation $\lambda = 488$ nm. Reprinted with permission from ref 52. Copyright 1998 Elsevier.

The difficulty in controlling the fullerene clusters dimensions, which can have a relatively large distribution of sizes, and the exact amount of fullerenes introduced in the matrix represents the main limit of the previous preparation methods.

The fullerene−host matrix interactions seem also to play a very important role. Several modifications of the photophysical properties of fullerenes in such porous media are, in fact, generally observed. Changes in the electronic states or even in the structure are induced in the fullerenes by interaction with the host matrix. Clear changes of the electronic state of C_{60} molecules in aerogel were observed. The formation of $C_{60}(OH)_x$ via direct interactions with the OH moiety on a pore surface of silica aerogels is likely to happen. The absence of quantum confinement confirms the structural changes; in fact, the PL spectra show only a very broad signal

around 2.2 eV without any blue shift. The intensity of the peak is much lower and without any sharp signal with respect to the samples where QC is clearly observed, and the PL curve seems insensitive to the fullerene concentration. The origin of the photoluminescent peak at 2.2 eV is explained by the presence of surface passivated species.

Another interesting phenomenon in fullerene-doped silica aerogels is the cluster generation by laser ablation.[54−58] In fullerene-doped aerogels, clusters of C_{60} and C_{70} together with fragmentation and aggregation of fullerenes are observed, upon irradiation by a XeCl excimer laser. The different aggregation state and distribution of fullerenes in the host matrix do not seem to produce the same effect, upon excimer laser irradiation, as that seen in carbon- or rhodamine 6G-doped aerogels. Laser energy is well adsorbed by fullerenes, but because the dopants are not evenly distributed on the silica network surface but incorporated in the pores as small aggregates, the energy absorption in the fullerene aggregate produces the vaporization of these particles without any transfer of energy to the matrix. After incorporation of fullerenes in two different aerogels, with different surface reactivity, under time-of-flight (TOF) laser desorption mass spectrometry, coalescence of fullerenes up to five C_{60} molecules is detected. This aggregation is not observed in nonreactive silica aerogels when chemical bonds with fullerenes are not formed. The formation of silica clusters is attributed to strong interactions between the fullerene molecules and reactive groups, such as −OH, on the porous matrix surface.

Silica aerogels doped with fullerenes were also tested as materials for energy storage applications.[59] Conductive aerogels are doped with fullerene whose charge-transfer properties are used in the process.

2.5. Fullerenes in Porous Inorganic Glasses. Fullerene-doped glasses were prepared by Joshi[60] et al., by contact of a commercial Corning 7930 Vycor glass, whose pore diameter is 4 nm, with solutions of C_{60} in toluene or CS_2. A fullerene concentration in the porous glass of 0.01 and 5 wt % can be reached by employing toluene or CS_2, respectively. Experiments of solvent extraction showed strong bonding of fullerenes with the pore walls.

3. Fullerenes and Their Derivatives in Sol−Gel Materials

The introduction of fullerenes in porous media is usually achieved, with the exception of aerogels, after material processing. This limitation is, of course, due to the requirement that the temperature necessary to prepare the matrix should not exceed that of fullerene degradation. Fullerene nanocomposites can, however, be prepared using host materials with low processing temperatures. One possibility is represented by organic polymers and another one by sol−gel materials. Organic polymers in combination with fullerenes, which are not included in this review, were widely investigated, and several applications were presented. Sol−gel materials are synthesized via soft chemistry from low temperatures and allow the preparation of host matrixes with very finely tuned properties. Sol−gel derived materials include porous inorganic glasses, inorganic oxides, hybrid organic−inorganic compounds, and aerogels. The literature on aerogel−fullerene nanocomposites was described in the previous section; in this part fullerene nanocomposites from sol−gel processing are reviewed.

3.1. Fullerene Derivatives for Applications in Sol−Gel Materials. Several kinds of inorganic or hybrid materials are commonly synthesized via sol−gel and easily processed especially as coatings. Sol−gel materials are also widely used as hosts for organic molecules because the doping media can be introduced a priori, before the material preparation, in the precursor sol and the temperatures to prepare the material can be low enough to avoid thermal degradation of the organic guest molecules. The only requirement is a good solubility in the polar solvents usually employed in sol−gel synthesis. C_{60} and C_{70} have, however, a very low solubility in these solvents, and only a relatively small amount of fullerenes can be introduced without aggregation or precipitation. Fundamental support is given by the functionalization chemistry of fullerenes.[61,62] The main task in functionalizing fullerenes for sol−gel materials is, of course, to increase the solubility in polar solvents, taking into account that some applications, such as optical limiting, require the introduction of significant volume fractions of fullerenes in the final material. At the same time a very homogeneous dispersion should be achieved without formation of aggregates, and the functionalized molecules must retain the properties of pristine fullerenes. Several solutions were developed to fulfill these requirements; in this section some basic principles and some examples of fullerene derivatives synthesized for specific application in sol−gel chemistry will be described.[63−65]

C_{60} shows a typical reactivity of electron-deficient olefins.[66,67] Adducts are readily formed upon reaction with radicals, some nucleophiles and carbenes. These reactions are exothermic and driven by the relief of strain in carbon double bonds. The spherical form of C_{60} imposes a deviation from planarity to carbon double bond and a stress is induced by pyramidalization of its sp^2 carbon atoms. The change from the stressed trigonal sp^2 to the less strained tetrahedral sp^3 state is associated with the reactivity of fullerenes. Two different types of carbon bonds were identified: short bonds (∼1.38 Å) that are located at the junctions of two six-membered rings (6,6 junctions), and long bonds (∼1.45 Å) at the junctions between a six- and a five-membered ring (5,6 junctions). 6,6 junctions, because of their higher electronic density, are a preferential site of attack for the reactants. Prato[63] classified the single addition products in different categories in relationship with the geometrical shape built on a 6,6 ring junction: open structures; three-member ring, which includes carbon and nitrogen insertions into a 5,6 ring junction; four-member ring; five-member ring; six-member ring (Figure 4).

Important families of fullerene derivatives used to fabricate sol−gel fullerene nanocomposites are methanofullerenes[61] (three-member ring group) and fulleropyrrolidines[64] (five-member ring group). In particular, much work was dedicated by Prato, Maggini, and coworkers to develop fulleropyrrolidine derivatives for specific sol−gel applications. Fullerene derivatives soluble in tetrahydrofurane (THF) were synthesized and their

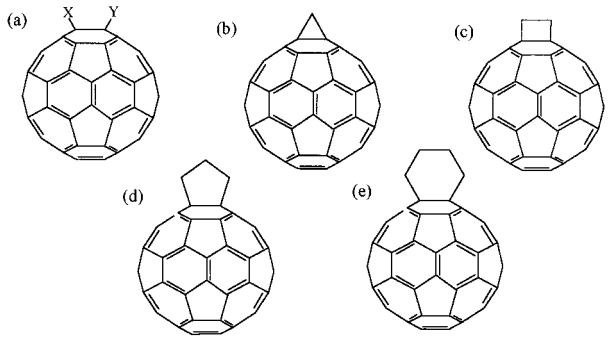

Figure 4. Geometrical shapes built on the 6,6 ring junction of C60: (a) open; (b) three-membered ring; (c) four-membered ring; (d) five-membered ring; (e) six-membered ring. Adapted from ref 63.

Table 1. Solubilities in THF of Fullerene Derivatives Used in Synthesis of Sol−Gel C_{60}−Nanocomposites (Adapted from ref 76)

DERIVATIVE		Solubility in THF (mg ml^{-1})
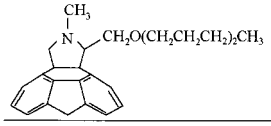	**1**	31
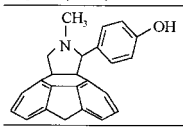	**2**	1.0
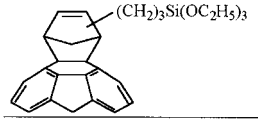	**3**	27
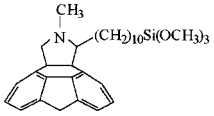	**4**	27
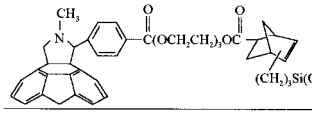	**5**	61
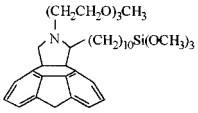	**6**	216
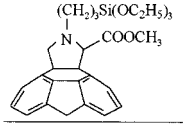	**7**	43

optical properties[68] tested for optical limiting applications.[17,69,70,88] Compounds **1** and **2** (Table 1) showed the possibility to be easily introduced in large amounts in sol−gel bulk and films.[17]

Another group of fulleropyrrolidines is characterized by a silicon alkoxide end group covalently linked to the fullerene[71−73] (compounds **3**−**7** in Table 1). This group of fullerenes is designed to have a solubilizing appendage together with a silicon alkoxide end group in order to be able to increase to amount of doping molecules in the matrix and to avoid aggregation effects that are detrimental for the nonlinear optical properties. Six-membered rings joined to 6,6 junctions can be obtained by the classical cycloaddition reactions to C_{60}. This synthesis has the advantage to allow the addition in one single step of the desired functionality, such as the silicon alkoxide end group, together with a solubilizing appendage. An alternative route to fulleropyrrolidine synthesis is the thermal ring opening of aziridines bearing electroattracting substituents in the presence of C_{60}. The derivatives show a solubility in THF ranging from 1 mg mL^{-1} for **2** to 216 mg mL^{-1} for **6**. The large solubility in THF and the presence of the trialkoxide groups allow sol−gel doped matrixes containing larger amounts and better dispersed fullerene derivatives to be maintained. In this group of fullerene derivatives, derivative **7** (indicated as FULP), a functionalized pyrrolidinofullerene generated by thermal ring opening of an azirine bearing both an electron attracting $-COOCH_3$ group and the silicon alkoxide functionality in the presence of C_{60}, can be easily produced in large scale and was chosen as the benchmark derivative for developing optical limiting applications at Padova University.

Methanofullerenes[74] for application in sol−gel materials were synthesized by the group of Los Alamos,[75] in particular phenyl-C_{61}-butyric acid choleteryl ester (PCB-CR) with the cholesteryl side chain attached via a 6−6 cycloaddition and 1-(3-methoxycarbonyl)propyl-1-phenyl-[6,6]-C_{61} (PCBM). The general advantage of methanofullerenes is their larger solubility in polar media. Felder[86] et al., however, observed micellar aggregation in aqueous NaOH solution of water-soluble methanofullerenes. Clustering was found also in THF and in ethanol, only in less polar solvent (CH_2Cl_2) the aggregation seems to be avoided.

Another interesting group of fullerene derivatives that has been applied in sol−gel processing is represented by fullerene amine derivatives.

Amine fullerene derivatives can be obtained by amination reactions of C_{60} with primary, secondary, or tertiary amines of the general type:

$$C_{60} + NHRR' \rightarrow H_xC_{60}(NRR')_x$$

$H_xC_{60}[NH(CH_2H_4O)_2H]_x$ or $H_xC_{60}[NH(CH_2)_3Si(OEt)_3]_x$, obtained by reacting C_{60} with 2-(2-aminoethoxy)ethanol or (3-aminopropyl)triethoxysilane, respectively, were obtained via this route by Tang[76] et al.

C_{60}-ethylenediamine and C_{60}-ethanolamine fullerene-amine derivatives[49] for applications in aerogels were prepared by reacting C_{60} with amines. The water solubility are larger for C_{60}-ethylenediamine. The same authors proposed the preparation of a fullerene-silane derivative, soluble in organic solvents such as methanol, THF, toluene, and methylene chloride, which can be used to produce inorganic aerogels containing fullerenes. This derivative is prepared by reaction of a C_{60}/C_{70} mixture with (3-aminopropyl)trimethoxysilane; the nominal composition of the compound was supposed to be C_{60}/C_{70} $[(NH_2(CH_2)_3Si(OMe)_3]_n$ with $n \approx 14$.

The same procedure to obtain a functionalized C_{60}/C_{70} mixture via a nucleophilic addition of (3-aminopropyl)trimethoxysilane to the C_{60}/C_{70} double bonds was used by Brunel[94] et al., for optical limiting applications of fullerenes.

Another fullerene derivative was prepared by West and co-workers,[77,78] who introduced alkoxysilyl groups by hydrosilylation of C_{60}. The resulting methyldiethoxysililated C_{60}, $H_nC_{60}[SiCH_3(OC_2H_5)]_{0.5}[SiCH_3(OC_2H_5)OSiHCH_3(OC_2H_5)]_{4.5}$, is soluble in benzene, hexane, and diethyl ether. The same authors have proposed an interesting route to prepare polymers with fullerene units as part of the polymeric chain. One example is the reaction of C_{60}, in the presence of a platinum catalyst, with two linear siloxane oligomers, $H(Si(CH_3)_2O)_3Si(CH_3)_2H$, to give a compound with about 12 siloxane chains per C_{60} unit. To develop a new route to obtain C_{60}-silica nanocomposites,[79] C_{60} was hydrosilylated with trichlorosilane, chlorodiphenylsilane, and dichlorophenylsilane using a platinum catalyst (H_2PtCl_2). The final formula of the compound, deduced from proton NMR, is $C_{60}\{Si(OC_2H_5)_3\}_{2.6}H_{2.6}$ or $C_{60}(SiPh_2Cl)_{3.2}H_{3.2}$.

An *o*-xylylene derivatization[80] was used to insert C_{60} as part of the side chain of poly(dimethylsiloxane) (PDMS). By this approach a fullerene content reaching 30 wt % PDMS was preferred because of its large chain mobility that is reflected in good solubility and thermal stability.

Another route is represented by fullerene complexes. Fullerene−tungsten complexes soluble in toluene,[81] $C_{60}[W(CO)_3diphos]$, were introduced in sol−gel matrixes; the solubility is, however, not larger than pristine fullerene and a final concentration of 2.47×10^{-5} mol L^{-1} was reported.

3.2. Fullerenes in Sol−Gel Inorganic Porous Media. Porous monolithic materials can be synthesized from acid and basic catalyzed sols of alkoxides. These porous materials are thermally stable and can be easily impregnated with C_{60} solutions.[82] Bulk material with a narrow pore size distribution and 2.8 nm average pore diameter was used by Zerda et al. to model the diffusion of C_{60} in cyclohexane (C_6H_{12}) and toluene ($C_6H_5CH_3$). The flow of fullerenes were mainly directed along the symmetry axis of the cylindrical pores, whereas in other directions small oscillations well approximated the motion. The diffusion of C_{60} was around 12 times slower than cyclohexane diffusion. This difference is due to steric hindrance effects, because the diameter of C_{60} is almost double that of cyclohexane.

An impregnation process was also followed by Schell,[83−85] et al. to prepare porous bulk xerogels doped with C_{60}. A basic and an acid synthesis have been used to produce silica samples with pore sizes of 3.8 and 6 nm, after firing. Solutions of C_{60} in toluene or chlorobenzene were used to impregnate the material, allowing a C_{60}:SiO_2 mass ratio of 0.03% in basic samples and 0.7% in acid samples. Attempts to embed methanofullerene derivatives failed because of the steric hindrance of the derivative and formation in solution of micellar aggregates.[86]

3.3. Fullerenes and Fullerene Derivatives in Inorganic and Hybrid Organic−Inorganic Sol−Gel Materials. The first fullerene silica sol−gel nanocomposite was prepared by Dai[16] et al. in 1992, mixing C_{70} in toluene with an acidic sol of tetraethyl orthosilicate ($Si(OCH_2H_5)_4$, TEOS). The amount of C_{70} introduced in the material was, however, very low, the C_{70}/SiO_2 molar ratio is, in fact, limited to 8×10^{-5}, and the same process to incorporate C_{60} failed.

In other attempts to introduce C_{60} in inorganic silica, bulk gels and[87,88] fullerene molecules were dissolved in chlorobenzene (C_6H_5Cl, (MCB)). MCB seems a better solvent to be employed in sol−gel synthesis because C_{60} has a good solubility in aromatic or halogenated aromatic solvents,[89] and it has a relatively low boiling point (132 °C) that can favor its evaporation during drying. A different behavior is reported if C_{60} is added in as-prepared or in well-reacted silica sols. Transparent films, 350 nm thick, can be obtained by this procedure with a molar ratio C_{60}/SiO_2 of 1.4×10^{-4}. A restriction to an extensive application of this procedure is, however, represented by the impossibility to obtain thick films even by multilayers and to produce uncracked silica bulk samples.

The attempts to introduce fullerenes in inorganic oxides followed the same strategy: to dissolve C_{60} or C_{70} in a suitable solvent, to mix in the precursor sol, and to obtain a gel that entraps the guest molecules. The low solubility of pristine fullerenes in polar solvents represents, however, a difficult limit to overcome, even if some special procedures are adopted. A better solubility is observed using aromatic or halogenated solvents, but the improvement is still too little to allow a significant increase of the amount of fullerenes introduced in the matrix. Another problem of this strategy is represented by uncontrolled clustering, which is a strong obstacle to any photonic application. Some small improvements are reported when a sonication process[90,91] is used during sol−gel synthesis or when small amounts of dimethyl phthalate (C_6H_4-1,2-$(CO_2CH_3)_2$) are added to increase the solubility of the system. In this case a concentration of C_{60} in silica−titania gel of 0.3 wt % was reported.[92]

Organic−inorganic hybrids are an alternative class of host materials for fullerenes prepared via sol−gel. These materials offer several advantages, thick layers, up to several micrometers per single deposition, are easily prepared, and dense materials can be obtained at a low processing temperature, usually lower than 150 °C. Hybrid materials are generally synthesized cohydrolyzing organically modified alkoxides with unmodified alkoxides. This opens the room to the preparation of a wide variety of materials whose properties result from a combination of those of inorganic oxides and organic polymers.

The approach to introduce fullerenes in hybrid matrixes does not differ much from the case of sol−gel inorganic materials. An example is given by C_{60}[93,94] simply added as a toluene solution to an acid catalyzed sol of zirconium butoxide ($Zr(OBu^t)_4$) and vinyltriethoxysilane ($H_2C{=}CHSi(OCH_2H_5)_3$). The concentration obtained in this case is, however, limited to a C_{60}/SiO_2 molar ratio of 6×10^{-6}.

A quite different route, via an impregnation process applied to multiphasic nanostructured composites, was used by Gvishi[95] et al. to synthesize fullerene-doped hybrid glasses. These materials have a nanoscale multiphasic structure and are prepared by impregnating highly porous silica bulk gels with methyl methacrylate ($H_2C{=}C(CH_3)CO_2CH_3$, (MMA)), which is immediately polymerized in situ. The same process can be employed to codope the material with another organic molecule with nonlinear optical properties. Bisbenzothiazole 3,4-

didecyloxythiophene (BBTDOT) was introduced in the matrix during MMA impregnation and remained entrapped in the matrix together with fullerenes.

An increased solubility of C_{60} is observed[18,79] when a benzene group is used as the functional group of the alkoxide. By use of phenyltriethoxysilane ($C_6H_5Si(OCH_2H_5)_3$, PTEOS) cohydrolyzed with TEOS, the solubility of C_{60} in the sol is increased and a 5×10^{-3} C_{60}:SiO_2 molar ratio is reached in spin-coated thin films. Fullerenes are not, however, completely dissolved in the solution; in fact, PL spectroscopy shows quantum size effects due to the presence of C_{60} clusters, which are composed, before the firing process, of around 60 C_{60} molecules. A comparison of the PL spectra of thin C_{60} films obtained by vapor deposition (peaks at 1.59 and 1.73 eV) and C_{60}-doped hybrid films (peaks at 1.58 and 1.66 eV) shows a shift that is an indication of quantum size effects due to clustering of C_{60} in the matrix. The size of the clusters, calculated on the basis of the square well potential, increases with the firing temperature due to diffusion of fullerenes in the matrix. The cluster dimension increases from an average of 60 C_{60} molecules, before firing, to around 240 molecules at 300 °C and 870 at 400 °C.

The same strategy can be used to introduce in hybrid materials C_{60}/C_{70} mixtures as pristine fullerenes or amine derivatives.[94] C_{60}/C_{70} mixtures, grafted with (3-aminopropyl)trimethoxysilane, was added to a sol of TEOS or methyltriethoxysilane and vinyltriethoxysilane prehydrolyzed in acidic conditions. The grafted C_{60}/C_{70} sample results are mechanically and chemically more stable with respect to the dispersed C_{60}/C_{70}.

An extensive investigation of fullerene and fullerene derivatives in hybrid organic−inorganic materials was reported by co-working research groups at the University of Padova. Adding C_{60} in chlorobenzene to an acid-catalyzed sol of TEOS and methyltriethoxysilane ($CH_3Si(OCH_2H_5)_3$, MTES),[96] 0.8 μm thick uncracked films and monoliths were obtained. The network of the host material is formed by an interconnected silica backbone modified by covalently linked methyl groups. The organic molecules modify the network structure, and thicker coatings with respect to inorganic sol−gel films, because the methyl groups reduce the stress in the drying stage, are obtained. The MTES−TEOS films are, however, not completely dense at the temperature used to process the films, around 200 °C, and the amount of C_{60} introduced in the material is still low with a C_{60}/SiO_2 molar ratio of 6×10^{-5}. Fullerene derivatives (**3**−**7**) in Table 1 can be embedded in the MTES−TEOS matrixes reaching a fullerene concentration of 1.66×10^{-3} mol L^{-1}.

Interesting results were obtained using as host matrix 3-(glycidoxypropyl)trimethoxysilane (GPTMS) hybrid materials. GPTMS is an organically modified alkoxide whose organic group covalently linked to the silicon atom contains an epoxide ring. A poly(ethylene oxide) chain is formed upon epoxy opening, in specific conditions of synthesis. Different from the case of MTES, in which organic groups are network modifiers, in GPTMS they are network formers. The material is formed by interconnected silica and poly(ethylene oxide) chains. Transition metal alkoxides, such Ti, Zr, or Al alkoxides, are the most common Lewis acids used to catalyze the epoxy polymerization.[109] These alkoxides play a double role because cohydrolyzed in acidic conditions with GPTMS become also part of the network affecting the final property of the host material, such as the refracting index. The materials prepared by GPTMS have, therefore, in specific conditions of synthesis when efficient epoxy ring opening is achieved, a network that is formed by organic and inorganic polymers. These materials are dense at low temperature, have low optical propagation losses[97,98] and high scratch resistance properties with mechanical properties close to hard plastics,[99] and are easily processed as bulk or thick coatings. Another important advantage is represented by their ability to be optically polished. In GPTMS hybrid films and bulks doped with fulleropyrrolidine,[69,70,73,88] derivative **7** in Table 1, it is found that when the derivative is directly bonded to the silica matrix, larger concentrations of fullerenes in sol−gel matrixes are achievable, about 8.5×10^{-4} C_{60}/SiO_2, 2 orders of magnitude larger than concentrations obtained with pristine C_{60}. By using monoadducts characterized by a silicon-alkoxide end group covalently linked to the fullerene, concentrations as large as 10^{-3} C_{60}/SiO_2 can be reached.

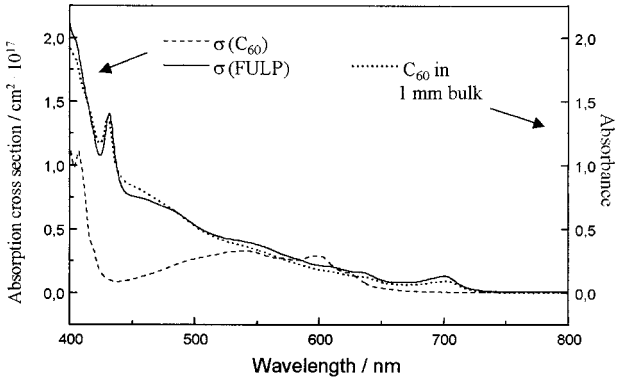

Figure 5. Linear absorption spectra of FULP (solid line) and C_{60} (dashed line) solutions in toluene (10 mm cuvette) and 1 mm FULP-doped GPTMS−ZrO_2 hybrid sol−gel bulk, with linear transmittance 0.80. Adapted from ref 23.

The nonlinear optical properties of the fulleropyrrolidines in sol−gel hybrid matrixes were extensively investigated.[100−107] The GPTMS matrixes were prepared by different epoxy ring polymerization catalysts,[108] in particular $Zr(OBu^t)_4$, BF_3, $SiCl_4$, $Ti(OBu^t)_4$, $TiCl_4$, and $Ti(OPr^i)_4$. Details of the synthesis can be found in refs 108 and 109. The linear absorption spectra of FULP and pristine C_{60} in toluene and FULP in a ZrO_2-GPTMS bulk matrix (1 mm thick) in the visible and near-infrared regions are reported in Figure 5.[102]

C_{60} in solution shows a broad absorption between 450 and 650 nm. In the same region, in addition to a narrow peak at 430 nm, FULP in toluene and in the sol−gel matrix shows a similar broad absorption that, however, is extended to 740 nm. Both the narrow peak and the additional deep-red absorption are typical of other 1,2 dihydrofullerenes.[110−112]

3.4. Optical Limiting Properties of Fullerene Sol−Gel Nanocomposites. The need for protecting optical sensors and human eyes from the damages induced by the high fluences of pulsed lasers has led to an increased attention to optical limiting materials. Optical limiting (OL) is observed when the optical

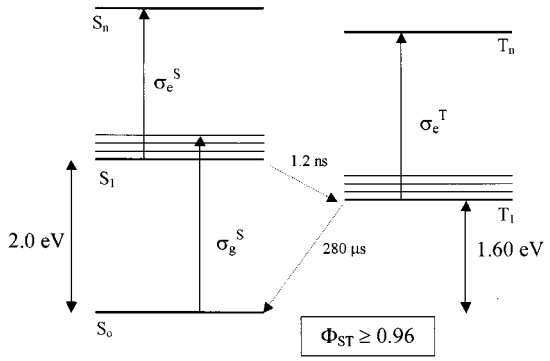

Figure 6. Five-level model of RSA in C_{60}.

transmission in a material decreases with increasing laser fluences. OL effects are observed in several materials and with different mechanisms, such as two-photon absorption, photorefraction, nonlinear scattering, and reverse saturable absorption (RSA).[113] Basically an optical limiter can be defined as a smart device that will limit the level of an optical signal that passes through it with an enhancing efficiency when the signal levels are increasing (details about OL systems and architectures for OL devices can be found in refs 114−116). The most promising results, in the visible range, are obtained with materials showing reverse saturable absorption. RSA occurs when a larger absorption from an excited state compared to that from the ground state is observed. Several organic molecules, such as metalloporphyrins and metallophthalocianines, have shown interesting OL properties in the green region, C_{60} and its derivatives represent an interesting class of molecules for optical limiting in the red region. C_{60} is characterized by a broad absorption spectrum with strong absorptions in the UV region and weak absorptions in the great part of the visible region, in this last region the first singlet excited state and the lowest energy triplet state show cross sections larger with respect to the ground state.

3.4.1. Reverse Saturable Absorption in Fullerenes. RSA in fullerenes is explained on the basis of a five levels model[117] (Figure 6). C_{60} shows singlet and triplet excited states; every electronic state is associated with a manifold of vibronic states. At low fluences, the ground state, S_0, is the only level significantly populated, at large fluences the first excited singlet state, S_1, becomes the populated state. The system in this state can either absorb another photon to rise to a higher singlet excited state, S_n, or cross to the lowest triplet excited state, T_1, which is energetically lower than S_1, with an intersystem crossing time τ_1. The population in T_1 can be excited to an upper triplet state, T_n, via one-photon absorption with a cross section, $\sigma_e T$, or relax to the ground state. The population in the excited states contributes to the total absorption of the system, and when $\sigma_e S > \sigma_g S$, the material becomes a reverse saturable absorber. The RSA mechanism is typical of moderate input fluences, while at large input fluences (larger than some J cm^{-2}) other mechanisms, such as nonlinear scattering, are activated, particularly in solution. In particular, a quantum yield close to unity for singlet-to-triplet population transfer (Φ_{ST}) makes the threshold for NL transmission one of the lowest known at the moment, while the broad absorption range in the visible spectra of the ground and triplet state makes C_{60} a potential broad band optical limiter.

The highest efficiency of an optical limiter based on RSA materials is reached when all the NLO molecules are pumped in the excited state to obtain the maximum absorption. There is, however, a limitation that is represented by the laser-induced damage of the solid-state host. The materials commonly available are, in fact, usually damaged before the input laser energy can reach a level to be able to pump efficiently all the molecules in the excited states. Near the damage threshold of the host matrix, the RSA materials are, therefore, only partially saturated, lowering the OL performances. To obtain efficient OL for practical applications, it is necessary, therefore, to reach a large concentration of fullerenes without aggregation in a material that should exhibit a high laser damage threshold.

The possibility to fabricate a solid-state optical limiter based on the RSA of C_{60} in sol−gel materials was widely investigated by several authors. These works can be grouped as a function of the type of fullerene employed to achieve OL performances: pristine fullerenes, soluble fullerene derivatives, and soluble fullerene derivatives terminated with silicon alkoxide groups. It is important to observe, reviewing the different works, that a quantitative comparison between the OL performances of the various C_{60}-doped glasses reported in the literature is quite difficult because a complete set of data is lacking, such as the molar fullerene concentration or laser beam dimension, or because of the heterogeneity of the experimental setup (wavelength, pulse duration, focal length). The presence of thermal effects, scattering, and other effects, particularly important in sol−gel matrixes due to fullerene aggregation and/or gel porosity, makes also difficult a direct comparison of the data reported by different authors.

3.4.2. OL from Fullerene and Soluble Fullerene Derivatives in Sol−Gel Materials. OL from fullerenes in SiO_2 matrixes was reported by McBranch[91] et al.; OL measurements (λ = 532 nm) on samples with two C_{60} concentrations exhibited RSA. The sample with a larger concentration shows a lower limiting fluence, as in toluene solution, due to C_{60} aggregation. The relative contributions of thermal effects, scattering losses, and RSA are not resolved, but hysteresis of the curves, depending if data are taken from low to high fluence or in the opposite direction, attributed to the thermal effect is observed. A better molecular dispersion was obtained by the same authors[74,75] after inclusion of the water-soluble fullerenes PCBR and PCBM in silica matrixes, as confirmed by relaxation dynamics measurements of the excited-state absorption and Raman spectra. The transmission at an incident energy of 3 mJ was more than a factor of 2 lower than for the sol−gel sample. This difference is attributed to thermal mechanisms that efficiently operate at high fluences for nanosecond pulses in solution and in the matrix cannot contribute.

OL is also observed in $C_{60}-SiO_2$ and $C_{60}-SiO_2-TiO_2$ nanocomposites,[92] with a large laser damage threshold. Enhanced OL performances incorporating methyl 1-phenyl-1-(9-hydro)fullerene derivatives in hybrid organic−inorganic matrixes are reported.

Brunel et al.[94] observed the strong effect produced on the RSA properties of fullerene from multifunctional-

ization with (3-aminopropyl)trimethoxysilane. A measure of the OL properties of dispersed C_{60}/C_{70} and grafted C_{60}/C_{70} in solution and in bulk gels has shown that the RSA characteristics of the functionalized fullerenes are deteriorated.

OL measurements on hybrid materials codoped with C_{60} and bisbenzothiazole 3,4-didecyloxythiophene (BBTDOT) were done by Prasad.[95] The reported transmittance for the C_{60}−BBTDOT composite is 0.92 at 800 nm and 0.30 at 532 nm. The OL measurements, interestingly, showed that the OL properties of C_{60} and BBDOT are combined in the material. BBDOT has strongly two-photon nonlinear absorption[118] (TPA) and OL behavior at 602 nm.[119] The C_{60}−BBTDOT nanocomposite shows OL at 532 nm due to C_{60} through RSA and at 800 nm due to BBTDOT through TPA.

OL measurements of C_{60} in porous gels[83−85] (with linear transmittance of about 30%) showed, by comparison between theoretical and experimental data, an irreversible bleaching of absorption at high excitation energies. Alternatively, a depopulation of the ground state can also explain the introduction of an intensity dependent two-photon absorption coefficient for the saturation effect. After inclusion of methanofullerene derivatives in silica matrixes a fast S_1-S_0 relaxation is observed, due to formation of micellar aggregates in the matrix and the OL performances upon nanosecond laser pulses are affected by these aggregates.[86]

Improved OL performances with respect to pristine C_{60} are observed after inclusion of C_{60} complexes in sol−gel films; the final amount of fullerene molecules in the matrix is, however, limited by the still low solubility of the complex in toluene.[81]

3.4.3. OL from Soluble Fullerene Derivatives Terminated with Silicon Alkoxide Groups in Sol−Gel Materials. Improved OL performances were observed in hybrid organic−inorganic sol−gel materials doped with soluble fullerene derivatives terminated with silicon alkoxide groups.[23,102,105−107] This family of materials presents the advantage to be doped with a very large amount of fullerene without showing any aggregation phenomenon because the fullerene derivatives are directly bonded to the matrix network. The application of this material in OL has two main advantages with respect to polymers, which are currently widely investigated for the same purpose,[120] a larger laser damage threshold, which directly increases the OL performances, and the possibility to be optically polished. An important finding is that some selected hybrid material can be dense at low temperatures, such as the hybrids from GPTMS. OL measurements in TEOS−MTES materials doped with several types of fullerene derivatives, even if possessing acceptable OL properties, show, however, some scattering effects attributed to residual porosity and aggregation of fullerenes that strongly reduce the OL efficiency.

The OL performances of FULP (derivative **7** in Table 1) upon incorporation in the hybrid matrix are very similar with respect to toluene solutions.[19,100,102]

As a consequence of the functionalization, the C_{60} simmetry is broken and a new transition band around 690 nm, accompanied by an absorption tail extended through the near-IR region (750 nm) are observed in FULP spectra.[121] Another difference between FULP and pristine C_{60} is the different triplet to triplet absorption, which peaks at 700 and 750 nm, respectively. Even if C_{60} and FULP have very similar optical properties, the efficiency of FULP in the red region of the spectrum are sensitively enhanced. Furthermore, because of the very low absorptions of C_{60} at 690 nm, much larger input fluences with respect to FULP are required to populate the triplet state. On the other hand, the linear properties of FULP are not affected by the incorporation in a solid matrix (Figure 5).

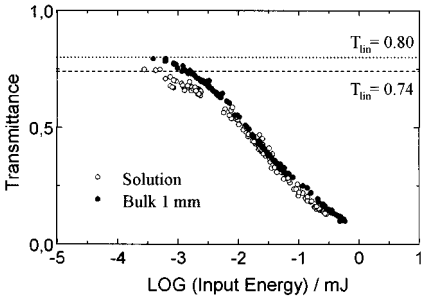

Figure 7. Optical limiting data: transmittance vs input energy (λ = 690 nm) of FULP toluene solution, with linear transmittance 0.74, and 1 mm FULP-doped GPTMS−ZrO_2 hybrid sol−gel bulk, with linear transmittance 0.80. Adapted from ref 23.

Table 2. Comparison of the Figures of Merit (FOM) for Fulleripyrrolidine Derivative (FULP) and Sn−Phthalocyanine (Sn−Pc)[a]

FULP (λ = 690 nm)	Sn−Pc (λ = 532 nm)
$\sigma_g = 1.1 \times 10^{-18}$ cm^2	$\sigma_g = 2.1 \times 10^{-18}$ cm^2
$\sigma_e = 6.2 \times 10^{-17}$ cm^2	$\sigma_e = 6.7 \times 10^{-17}$ cm^2
(FOM) $\sigma_e - \sigma_g = 6.1 \times 10^{-17}$ cm^2	$\sigma_e - \sigma_g = 6.5 \times 10^{-17}$ cm^2
Φ = 0.85−0.90	Φ = 0.55
FS = 0.31 J cm^{-2}	FS = 0.33 J cm^{-2}
T_{ph} = 39%	T_{ph} = 20%
(T_{lin} = 71% at 690 nm)	(T_{lin} = 71% at 532 nm)

[a] σ_e = triplet state absorption cross section, Φ = fluence, σ_g = ground state absorption cross section, FS = saturation fluence, T_{ph}= photopic transmission, T_{Lin} = linear transmittance. (Data are from ref 19.)

OL data of a 10 mm FULP solution in toluene, with linear transmittance T_{lin} = 0.74, and of the bulk sample at 690 nm are reported in Figure 7.

The OL performances of FULP in the sol−gel matrix are very similar to those in solution, as was experimentally confirmed. Inclusion of fullerene derivatives in a solid matrix without affecting the good NL properties of the molecules in solutions can be, therefore, reached with sol−gel processing of hybrid materials.

An interesting comparison of the optical properties of FULP and with those of Sn−phthalocyanine (Sn−Pc)[114−116] at 532 nm, which is considered to be one of the best RSA materials in the green region, allowed evaluation of the OL potentialities of FULP. The figure of merit (FOM) and the saturation fluence FS (FS = $h\nu/\Phi\sigma_g$, with Φ = fluence and σ_g = ground-state absorption cross section) were used for the comparison.[23] The data (Table 2) showed that at 690 nm FULP has almost the same performances as Sn−Pc at 532 nm. If, however, also considered is the "photopic transmission", T_{ph}, which is an important parameter to evaluate the efficiency of an optical limiter, FULP shows the advantage of a large T_{ph} in solutions with high linear transmittance. This is an indication that high concentrations of

FULP can still give a reasonable visibility loss with a corresponding increased efficiency for RSA optical limiting.

4. Glass and Ceramics Fullerene Nanocomposites

The possibility of introducing fullerenes in materials processed at high temperature, such as optical glasses, was demonstrated by Lin and co-workers.[122−125] Raw materials of phosphate and fluorophosphates glasses have been added to a mixture of C_{60}/C_{70} fullerenes, fired 1 h in a sealed device at 1200 K and slowly cooled. The sealed system avoided degradation of fullerenes, and up to 0.1 wt % of C_{60}/C_{70} can be introduced in the glass. Attempts to reach larger concentrations produce cracks in the glass during cooling, and the best quality glasses are obtained with even lower concentrations, typically 0.01 wt %. Several changes in the glass properties are observed, the most noticeable is a blue shift in the UV absorption edge attributed to changes in the energy gap between bonding and antibonding orbitals of nonbridging oxygens in glass after introduction of fullerenes. Fullerenes form aggregates of different dimensions and inhomogeneous distribution within the glass matrix. This is reflected in changes of mechanical properties and photoluminescence, in particular an increase in Vickers hardness and the arise of a white broad PL band. The PL is attributed to fullerenes confined or linked via −C−O bonds to $-[PO_4]-$ tetrahedra; these fullerenes form islands randomly distributed in the glass network. As a consequence of fullerene aggregation, breaking in the glass centrosymmetric structure near the self-assembled fullerene aggregates produces macroscopic second-order nonlinearities. A sensitive enhancement, close to 2 orders of magnitude, of the second harmonic generation is observed close to these aggregates.

A different route to introduce fullerenes into ceramics materials was followed by Miyazawa[126] et al. Zirconia powders were doped with C_{60} and sintered to obtain a bulk material. This process, however, produces the partial transformation of C_{60} into graphite and amorphous carbon thin layers on the surface of ZrO_2 grains and only a small amount of C_{60} is retained in the sintered specimens. Similarly, attempts to introduce C_{60} in ZrO_2 via sol−gel synthesis, after thermal treatment of the powders at 500 °C gives a partial transformation of fullerenes into graphite, n-diamond, and carbyne.[127]

5. Outlook

A large variety of fullerene organic−inorganic nanocomposite materials have been studied and successfully prepared in the past few years following the booming research on fullerenes. Fullerenes have been introduced in materials with different properties and characteristics showing several potential applications in materials science while functionalization chemistry of fullerenes has emerged as a key tool to design the material properties as a function of the application. The low solubility of fullerenes in polar media and the high tendency to form aggregates have represented the main obstacle in the development of devices based on fullerene itself. Even if much academic research has been addressed to these topics, it seems from the state of the present knowledge that functionalized fullerenes represent the main route to develop materials for practical applications. It is also clear that once entrapped within the host matrix, the nature of the surrounding media and the aggregation state have a strong influence on the fullerene properties and the reciprocal dual interaction matrix−fullerene cannot be generalized and must be studied case by case. Two main applications have been explored, photoluminescent materials and optical limiters, with the last one representing the most studied fullerene nanocomposite and likely the closest to commercial applications. Many of the potential applications of fullerenes are, however, still to be exploited, and this represents the challenge of the future.

Acknowledgment. A grateful thank is due to Professor M. Prato and M. Maggini whose deep knowledge of fullerene chemistry is a continuous stimulus to develop new materials from fullerenes and to Professor R. Bozio, M. Meneghetti, and R. Signorini for their invaluable optical modeling and characterization. Professor M. Guglielmi is also acknowledged for helpful discussions. The European Commission (DG XII), through contracts BRPR-CT97-0564 and CNR L.95/95 is acknowledged for financial support.

References

(1) Kroto, H. W.; Heath, J. R.; O'Brien, S. C.; Curl, R. F.; Smalley, R. E. *Nature* **1985**, *318*, 162.
(2) Krätschmer, W.; Lamb, L. D.; Fostiropoulos K.; Huffman, D. R. *Nature* **1990**, *347*, 354.
(3) Gust, D.; Moore, T. A.; Moore, A. L., *J. Photochem. Photob. B*: *Biology* **2000**, *58*, 63.
(4) Guldi, D. M. *Chem. Commun.*, **2000**, 321.
(5) Hudspeth, Q.; Hebard, A. F. *J. Supercond.* **2000**, *13*, 829.
(6) Dresselhaus, M. S.; Dresselhaus, G. *Nanostruct. Mater.* **1997**, *9*, 32.
(7) Mirkin, C. A.; Caldwell, W. B. *Tetrahedron* **1996**, *14*, 5113.
(8) Hirsch, A. *Adv. Mater.* **1993**, *11*, 859.
(9) Keizer, P. N.; Morton, J. R.; Preston, K. F.; Sudgen, A. K., *J. Phys. Chem.* **1991**, *95*, 7177.
(10) Anderson, M. W.; Shi, J.; Leigh, D. A.; Moody, A. E.; Wade, F. A.; Hamilton, B.; Carr, S. W. *J. Chem. Soc., Chem. Commun.* **1993**, 533.
(11) Hamilton, B.; Rimmer, J. S.; Anderson, M.; Leigh, D. *Adv. Mater.* **1993**, *5*, 583.
(12) Lamrabte, A.; Janot, J. M.; Elmidaoui, A.; Seta, P.; De Ménorval, L. C.; Backov, R.; Rozière, J.; Sauvajol, J. L.; Allègre, J. *Chem. Phys. Lett.* **1998**, *295*, 257.
(13) Lamrabte, A.; Janot, J. M.; De Ménorval, L. C.; Backov, R.; Rozière, J.; Sauvajol, J. L.; Allègre, J.; Seta, P. *Synth. Met.* **1999**, *103*, 2426.
(14) Gügel, A.; Müllen, K.; Reichert, H.; Schmidt, W.; Schön, G.; Schüth, F.; Spickermann, J.; Titman, J.; Unger, K., *Angew. Chem., Int. Ed. Engl.*, **1993**, *32*, 556.
(15) Annen, M. J.; Young, D.; Daviers, M. E.; Cavin, O. B.; Hubbard, C. R. *J. Phys. Chem.* **1991**, *95*, 1380.
(16) Dai, S.; Compton, R. N.; Young, J. P.; Mamantov, G. *J. Am. Ceram. Soc.* **1992**, *75*, 2865.
(17) Maggini, M.; Scorrano, G.; Prato, M.; Brusatin, G.; Innocenzi, P.; Guglielmi, M.; Renier, A.; Signorini, R.; Meneghetti, M.; Bozio, R. *Adv. Mater.* **1995**, *7***,** 404.
(18) Hasegawa, I.; Shibusa, K.; Kobaysahi, S.; Nonomura, S.; Nitta, S. *Chem. Lett.* **1997**, 995.
(19) Sariciftci, N. S.; Smilowitz, L. S.; Heeger, A. J.; Wuld, F. *Synth. Met.* **1993**, *59*, 333.
(20) Leach, S.; Vervloet, M.; Depres, A.; Breheret, E.; Hare, J. P.; Tennis, T. J.; Kroto, H. W.; Taylor, R.; Walton, D. R. M. *Chem. Phys.* **1992**, *160*, 451.
(21) Ruoff, R. S.; Tse, D. S.; Malhotra, R.; Lorents, D. C. *J. Phys. Chem.* **1993**, *97*, 3379.
(22) Bensasson, R. V.; Bienvenue, E.; Dellinger, M.; Leach, S.; Seta, P. *J. Phys. Chem.* **1994,** *98*, 3492.
(23) Signorini, R.; Meneghetti, M.; Bozio, R.; Maggini, M.; Scorrano, G.; Prato, M.; Brusatin, G.; Innocenzi, P.; Guglielmi, M. *Carbon* **2000**, *38*, 1653.

(24) Van den Heuvel, D. J.; Chan, I. Y.; Groenen, E. J. J.; Matsushita, M.; Schmidt, J.; Meijer, G. *Chem. Phys. Lett.* **1995**, 233.
(25) Guess, W.; Feldmann, J.; Gobel, E. O.; Taliani, C.; Mohn, H.; Muller, W.; Haussler, P.; Ter Meer, H. U. *Phys. Rev. Lett.* **1994**, 72, 2644.
(26) Yang, L.; Dorsinville, R. *Opt. Commun.* **1996**, *124*, 45.
(27) Gu, G.; Ding, W.; Cheng, G.; Zang, W.; Zen, H.; Du, Y. *Appl. Phys. Lett.* **1995**, *67*, 327.
(28) Gu, G.; Ding, W.; Cheng, G.; Zang, W.; Du, Y., Yang, S., *Chem. Phys. Lett.* **1997**, *270*, 135.
(29) Zhenyu, Z.; Warren, R.; Fehlner, J. R. USA Pat. No. U.S. 5,-364,993, 1994.
(30) Saito, R.; Dresselhaus, G.; Dresselhaus, M. S. *Physical properties of carbon nanotubes*; Imperial College Press: London, 1998.
(31) (a) Tang, Z. K.; Sun, H. D.; Wang, J.; Chen, J.; Li, G. *Appl. Phys. Lett.* **1998**, *73*, 2287. (b) Launois, P.; Moret, R.; Le Bolloćh, D.; Albouy, P. A.; Tang, Z. K.; Li, G.; Chen, J. *Solid State Commun.* **2000**, *116*, 99.
(32) a) Kresge, C. T.; Lenowicz, M. F.; Roth, W. J.; Vartuli, J. C.; Beck, J. S. *Nature* **1992**, *359*, 710. (b) Beck, J. S.; Vartuli, J. C.; Roth, W. J.; Lenowicz, M. F.; Kresge, C. T.; Schmitt, K. D.; Chu, C. T.; Olson, D. H.; Sheppard, E. W.; McCullen, S. B.; Higgins, K. D.; Schlenker, J. L. *J. Am. Chem. Soc.* **1992**, *114*, 10834.
(33) Stein, A.; Melde, B. J.; Schroden, R. C. *Adv. Mater.* **2000**, *12*, 1403.
(34) a) Yanagisawa, T., Shimizu, T.; Kuroda, K.; Kato, C. *Bull. Chem. Soc. Jpn.* **1990**, *63*, 988. (b) Inagaki, S.; Fukushima, Y.; Kuroda, K. *J. Chem. Soc., Chem. Commun.* **1993**, 680.
(35) Rachdi, F.; Hajji, L.; Goze, C.; Jones, D. J.; Maireles-Torres, P.; Rozière, J. *Solid State Commun.* **1996**, *100*, 237.
(36) Gu, G.; Ding, W.; Du, Y.; Huang, H.; Yang, S. *Appl. Phys. Lett.* **1997**, *70*, 2619.
(37) Chen, J. S.; Li, Q. H.; Ding, H.; Pang, W. Q.; Xu, R. R. *Langmuir* **1997**, *13*, 2050.
(38) Piwonski, I.; Zajac, J.; Jones, D. J.; Rozière, J.; Partyka, S.; Plaza, S. *Langmuir* **2000**, *16*, 9488.
(39) Piwonski, I.; Zajac, J.; Jones, D. J.; Rozière, J.; Partyka, S. *J. Mater. Chem.* **1998**, *8*, 17.
(40) Govindaraj, A.; Nath, M.; Eswaramoorthy, M. *Chem. Phys. Lett.*, **2000**, *317*, 35.
(41) Kobayashi, N.; Nitta, S.; Habuchi, H.; Yasui, T.; Itoh, T.; Nonomura, S. *Mol. Cryst. Liq. Cryst.* **2000**, *340*, 781.
(42) Fukuoka, A.; Fujishima, K.; Chiba, M.; Yamagishi, A.; Inagaki, S.; Fukushima, Y.; Ichikawa, M. *Catal. Lett.* **2000**, *68*, 241.
(43) Tachibana, J.; Chiba, M.; Ichikawa, M.; Imamura, T.; Sasaki, Y. *Supramol. Sci.* **1998**, *5*, 281.
(44) Drljaca, A.; Kepert, C.; Spiccia, L.; Raston, C. L.; Sandoval, C. A., Smith, T. D. *Chem. Commun.* **1997**, 195.
(45) Yan, F.; Bao, X. M.; Wu, X. W.; Chen, H. L. *Appl. Phys. Lett.* **1995**, *67*, 3471.
(46) Wu, X. L.; Yan, F.; Bao, X. M.; Tong, S.; Siu, G. G.; Jiang, S. S.; Feng, D. *Phys. Lett. A* **1997,** *225*, 170.
(47) Yamaguchi, S.; Miyoshi, *Surf. Sci.* **1996**, *357*−*358*, 283.
(48) (a) Fricke, J. *Aerogels*; Fricke, J., Ed.; Springer: Berlin, 1986. (b) Fricke, J. *Sci. Am.* **1988**, *256*, 92.
(49) Bell, W. L.; Jiang, Z.; Dietz, S. D. *Fullerenes*: *Recent Advances in the Chemistry and Physics of Fullerenes and Related Materials*; Kadish, K. M., Ruoff, R. S., Eds.; The Electrochem. Soc. Inc.: Pennington, NJ, 1994; Vol. 94−24, p 92.
(50) Zhu, L.; Li, Y.; Wang, J.; Shen, J. *Chem. Phys. Lett.* **1995**, *239*, 393.
(51) Zhu, L.; Li, Y.; Wang J.; Shen, J. *J. Appl. Phys.* **1995**, *77*, 2801.
(52) Shen, J.; Wang, J.; Zhou, B.; Deng, Z.; Weng, Z.; Zhu, L.; Zhao L.; Li, Y. *J. Non-Cryst. Solids* **1998**, *225*, 315.
(53) Zhu, L.; Ong, P. P.; Shen J.; Wang, J. *J. Phys. Chem. Solids* **1998,** *59*, 819.
(54) Zhao, L.; Zhu, L.; Liu, L.; Zhang, J.; Li, Y.; Zhang, B.; Shen, J.; Wang, J. *Chem. Phys. Lett.* **1996**, *255*, 142.
(55) Zhao, L.; Shen, J., Zhang, R. J.; Wang, J.; Li, Y. *Chin. J. Lasers* **1996**, *A23*, 1011.
(56) Wang, J.; Shen, J.; Zhou, B.; Deng, Z.; Zhao, L.; Li, Y. *Nanostruct. Mater.* **1998**, *10*, 909.
(57) Zhu, L.; Ong, P. P.; Zhao, L.; Zhang, R. J.; Li, Y. F. *Appl. Phys. B*: *Lasers Opt.* **1998**, *66*, 99.
(58) Zhou, B.; Wang, J.; Zhao, L.; Shen, J.; Deng, Z.; Li, Y. *J. Vac. Sci. Technol.* **2000**, *18*, 2001.
(59) Lamb, L. D.; Huffman, D. R. US Pat. No. US 5,698,140, 1997.
(60) Joshi, M. P.; Kukreja, L. M., Rustagi, K. C., *Appl. Phys. A*: *Mater. Sci. Process.* **1997**, *65*, 5.
(61) Diederich, F.; Issaci, L.; Philp, D. *Chem. Soc. Rev.* **1994**, *23*, 243.
(62) *The Chemistry of Fullerenes*; Taylor, R., Ed.; World Scientific: Singapore, 1995.
(63) Prato, M. *J. Mater. Chem.* **1997,** *7*, 1097.
(64) Prato, M.; Maggini, M. *Acc. Chem. Res.* **1998**, *31*, 519.
(65) Diederich, F.; Thilgen, C. *Science* **1996**, *271*, 317.
(66) Hirsch, A. *The Chemistry of the Fullerenes*; Thieme: Stuttgart, Germany, 1994.
(67) Wudl, F. *Acc. Chem. Res.* **1992**, *25*, 157.
(68) Signorini, R.; Zerbetto, M.; Meneghetti, M.; Bozio, R.; Maggini, M.; De Faveri, C.; Prato, M.; Scorrano, G. *J. Chem. Soc., Chem. Commun.* **1996**, 1891.
(69) Maggini, M.; Scorrano, G.; Prato, M.; Brusatin, G.; Innocenzi, P.; Guglielmi, M.; Meneghetti, M.; Bozio, R. Fullerenes: recent advances in the chemistry and physics of fullerenes and related materials. *Electrochem. Soc. Proc.* **1995**, *95*−*10*, 84.
(70) Bozio, R.; Meneghetti, M.; Signorini, R.; Maggini, M.; Scorrano, G.; Prato, M.; Brusatin, G.; Guglielmi, M. *Photoactive Organic Materials*; Kajzar, F., et al., Eds.; Kluwer Academic Publishers: Hingham, MA, 1996; pp 159−174.
(71) Maggini, M.; De Faveri, C.; Scorrano, G.; Prato, M.; Brusatin, G.; Guglielmi, M.; Meneghetti, M.; Signorini, R.; Bozio, R. *Chem.*−*Eur. J.* **1999**, *5*, 2501.
(72) Maggini, M.; Scorrano, G.; Prato, M.; *J. Am. Chem. Soc.* **1993**, *115*, 9798.
(73) Signorini, R., Zerbetto, M.; Meneghetti, M.; Bozio, R.; Maggini, M.; Scorrano, G.; Prato, M.; Brusatin, G.; Menegazzo, E.; Guglielmi, M. Fullerenes and Photonics III. *SPIE* **1996**, *2854***,** 130.
(74) Hummelen, J. C.; Knight, B.; Lepec, F.; Wudl, F. *J. Org. Chem.* **1995**, *60*, 532.
(75) McBranch, D.; Klimov, V.; Smilowitz, L.; Grigorova, M., Robinson, J. M.; Koskelo, A.; Mattes, B. R. *SPIE* **1996**, *2854*, 140.
(76) Wu, X. Z.; Yu, N. T.; Leung. S. M.; Peng, H.; Tang B. Z. US. Pat. No. U.S. 6,066,272, 2000.
(77) West, R.; Oka, K.; Miller, M.; Gunji, T.; Takahashi, H.; Skrupky, R. L.; Wang, Y. *Proceedings of the 26th Silicon Symposium*; IUPUI, Indianapolis, 1993; p C-1.
(78) West, R.; Oka, K.; Takahashi, H.; Miller, M.; Gunji, T. *Inorganic and Organometallics Polymers II*: *Advanced Materials and Intermediates*; ACS Symposium Series 572; American Chemical Society, Washington, DC, 1994; p 92.
(79) Hasegawa, I.; Nonomura, S. *J. Sol*−*Gel Sci. Technol.* **2000,** *19*, 297.
(80) Kraus, A.; Müllen, K. *Macromolecules* **1999**, *32***,** 4214.
(81) Dou, K.; Du, J. Y.; Knobbe, E. T. *J. Lumin.* **1999**, *83*−*84***,** 241.
(82) Zerda, T. W.; Broda, A.; Coffer, J. *J. Non-Cryst. Solids* **1994**, *168*, 33.
(83) Schell, J.; Brinkmann, D.; Ohlmann, D.; Levy, R.; Joucla, M.; Rehspringer, J. L.; Serughetti, J.; Bovier, C. *J. Chem. Phys.* **1998**, *108*, 8599.
(84) Schell, J.; Ohlmann, D.; Brinkmann, D.; Levy, R.; Joucla, M.; Rehspringer, J. L.; Honerlage, B. *J. Chem. Phys.* **1999**, *111*, 5929.
(85) Schell, J.; Ohlmann, D.; Honerlage, B.; Levy, R.; Joucla, M.; Rehspringer, J. L.; Serughetti, J.; Bovier, C. *Carbon* **1998**, *36*, 671.
(86) Felder, D.; Guillon, D.; Lévy, R.; Mathis, A.; Nicoud, J.-F.; Nierengarten, J. F.; Rehspringer, J. L.; Schell, J. *J. Mater. Chem.* **2000**, *10*, 887.
(87) Brusatin, G.; Guglielmi, M.; Bozio, R.; Meneghetti, M.; Signorini, R.; Maggini, M.; Scorrano, G.; Prato, M. *J. Sol*−*Gel Sci. Technol.* **1997**, *8*, 609.
(88) Prato, M.; Maggini, M.; Scorrano, G.; Brusatin, G.; Innocenzi, P.; Guglielmi, M.; Meneghetti, M.; Bozio, R. *Mater. Res. Soc. Symp. Proc.* **1995**, *359*, 351.
(89) Ruoff, R. S.; Tse, D. S.; Malhotra, R.; Lorents, D. C. *J. Phys. Chem.* **1993**, *97*, 3379.
(90) Mattes, B. R.; McBranch, D. W.; Robinson, J. M.; Love, S. P.; Koskelo, A. C., US Pat. No. US 5,420,081, 1995.
(91) McBranch, D. W.; Mattes, B. R.; Koskelo, A.; Robinson, J. M.; Love, S. P. Fullerenes and photonics. *SPIE* **1994**, *2284*, 15.
(92) Zhu Congshan; Xia Haiping; Gan Fuxi *Proc. Int. Cong. Glass, XVII* **1995**, *4***,** 204.
(93) Bentivegna, F.; Canva, M.; Georges, P.; Brun, A.; Caput, F.; Malier, L.; Boilot, J. P. *Appl. Phys. Lett.*. **1993**, *62*, 1721.
(94) Brunel, M.; Canva, M.; Brun, A.; Chaput, F.; Malier, L.; Boilot, J. P. Materials for Optical Limiting. *Mater. Res. Soc. Symp. Proc.* **1995,** *374***,** 281.
(95) Gvishi, R.; Bhalwalkar, J. D.; Kumar, N. D.; Ruland, G.; Narang, D.; Prasad, P. N.; Reinhardt, B. A. *Chem. Mater.* **1995**, *7*, 2199.
(96) Innocenzi, P.; Abdirashid, M. O.; Guglielmi, M. *J. Sol-Gel. Sci. Technol.* **1994**, *3*, 47.
(97) Innocenzi, P.; Martucci, A.; Guglielmi, M.; Armelao, L.; Battaglin, G.; Pelli, S.; Righini, G. C. *J. Non-Cryst. Solids* **1999**, *259*, 189.
(98) Brusatin, G.; Guglielmi, M.; Innocenzi, P.; Martucci, A.; Scarinci, G. *J. Electroceram.* **2000**, *4*, 151.
(99) Innocenzi, P.; Esposto, M.; Maddalena, A. *J. Sol*−*Gel Sci. Technol.* **2001**, *20*, 293.
(100) Signorini, R.; Meneghetti, M.; Bozio, R.; Maggini, M.; Scorrano, G.; Prato, M.; Brusatin, G.; Innocenzi, P. *Nato ASI Series*, 1999 Menton, France, in print.
(101) Signorini, R.; Sartori, S.; Meneghetti, M.; Bozio, R.; Maggini, M.; Scorrano, G.; Prato, M.; Brusatin, G.; Guglielmi, M. *Nonlinear Opt.* **1999**, *21*, 143.
(102) Reference 23.
(103) Signorini, R.; Tonellato, A.; Meneghetti, M.; Bozio, R.; Prato, M.; Maggini, M.; Scorrano, G.; Brusatin, G.; Innocenzi, P.; Guglielmi, M. *Nonlinear Opt.* **2001**, 193.

(104) Brusatin, G.; Guglielmi, M.; Innocenzi, P.; Bozio, R.; Signorini, R.; Meneghetti, M.; Maggini, M.; Scorrano, G.; Prato, M. *SPIE* **1999**, *3803*, 90.
(105) Innocenzi, P.; Brusatin, G. Guglielmi, M. Signorini, R. Bozio, R. Maggini, M. *J. Non-Cryst. Solids* **2000**, *265*, 68.
(106) Innocenzi, P.; Brusatin, G.; Guglielmi, M.; Signorini, R.; Meneghetti, M.; Bozio, R.; Maggini, M.; Scorrano, G.; Prato, M. *J. Sol−Gel Sci. Technol.* **2000**, 19, 263.
(107) Brusatin, G.; Innocenzi, P.; Guglielmi, M.; Signorini, R.; Bozio, R. *Nonlinear Opt.* **2001**, 259.
(108) Innocenzi, P.; Brusatin, G.; Guglielmi M.; Bertani, R. *Chem. Mater.* **1999**, *11*, 1672.
(109) Innocenzi, P.; Brusatin G.; Babonneau, F. *Chem. Mater.* **2000**, *12*, 3726.
(110) Anderson, J. L.; An, Y. Z.; Rubin, Y.; Foot, C. S. *J. Am. Chem. Soc.* **1994**, *116*, 9763.
(111) Bensasson, R. V.; Bienvenue, E.; Janot, J. M.; Leach, S.; Seta, P.; Schuster, D. I.; Wilson, S. R.; Zhao, H. *Chem. Phys. Lett.* **1995,** *245*, 566.
(112) Williams, R. M.; Zwier, J. M.; Verhoeven, J. W. *J. Am. Chem. Soc.* **1995**, *117*, 4093.
(113) (a) *SPIE*, Vol. 3798, *Power limiting materials and devices*, Ed. By C. M.Lawson, 1999. (b) Proceedings of the International Symposium on Optical Power Limiting, Venice 2000, *Nonlinear Opt.*, in press.
(114) Miles, P. A. *Appl. Opt.* **1994**, *33*, 6965.
(115) Xia, T.; Hagan, D. J.; Dogariu, A.; Said A. A.; Van Stryland, E. W. *Appl. Opt.* **1997**, *36*, 4110.
(116) Miles, P. A. *Appl. Opt.* **1999**, *38*, 566.
(117) Kost, A., Tutt, L.; Klein, M. B.; Dougherty, T. K.; Elias, W. E. *Opt. Lett.* **1993**, *18*, 334.
(118) He, G. S.; Zu, G. C.; Prasad, P. N.; Reinhardt, B. A.; Bhatt, J. C.; Dillard, A. G. *Opt. Lett.* **1995**, *20*, 437.
(119) He, G. S.; Gvishi, R.; Prasad, P. N.; Reinhardt, B. A.; Bhatt, J. C.; Dillard, A. G. *Opt. Commun.* **1995**, *117*, 133.
(120) Tang, B. Z.; Xu, H.; Lam, J. W. Y.; Lee, P. P. S.; Xu, K.; Sun, Q.; Cheuk, K. K. L. *Chem. Mater.* **2000**, *12*, 1446.
(121) Meneghetti, M.; Signorini, R.; Zerbetto, M.; Bozio, R.; Maggini, M.; Scorrano, G.; Prato, M.; Brusatin, G.; Menegazzo E.; Guglielmi, M. *Synth. Met.* **1997,** *86*, 2353.
(122) Lin, F.; Mao, S.; Meng, Z.; Zeng, H.; Qiu, J.; Yue, Y.; Guo, T. *Appl. Phys. Lett.* **1994**, *65*, 2522.
(123) Lin, H.; Taheri, B.; Jia, W.; Lin, F.; Mao, S. *Appl. Phys. Lett.* **1996**, *68*, 1570.
(124) Liu, H.; Jia, W.; Lin, F.; Mao, S. *J. Lumin.* **1996**, *66&67*, 128.
(125) Zeng, H.; Sun, Z.; Segawa, Y.; Lin, F.; Mao, S.; Xu, Z.; Tang, S. H. *J. Phys. D*: *Appl. Phys.* **2000**, *33*, L93.
(126) Miyazawa, K.; Yano, J.; Honma, I.; Akaishi, M. *J. Am. Ceram. Soc.* **2000**, *83*, 2315.
(127) Miyazawa, K.; Takahashi, T.; Ogawa, K.; Kuzumaki, T.; Ito, K. *Processing and Fabrication of Advanced Materials VI*; Khor, K. A., Srivatsan, T. S., Moore, J. J., Eds.; The Institute of Materials: London, 1998; Vol.1, p 775.

CM0110223